

Design of Temperature Control System on UV Weathering Chamber Based on PID (Proportional, Interval, and Derivative)

Zakaria¹, Dedik Romahadi^{1,2*}, Muhamad Fitri¹

¹Department of Mechanical Engineering, Faculty of Engineering, Universitas Mercu Buana, Kembangan, Jakarta Barat, 11650, Indonesia

²Department of Manufacturing Engineering, Faculty of Engineering, Beijing Institute of Technology, Beijing, 100081, China

*E-mail: dedik.romahadi@mercubuana.ac.id

Abstract--The influence of high temperature and exposure to ultraviolet (UV) radiation from sunlight, rain, and humidity causes damage to the composite material and consequently, reduces its mechanical performance. Weathering experiments can be carried out outdoors or under laboratory conditions. Material degradation tests can be carried out directly using natural conditions or laboratory test equipment that artificially simulates natural conditions. An automatic temperature control system is needed to keep the setpoint stable during the degradation test. The controller on the system uses Arduino based on Proportional, Interval, and Derivative (PID). There are three types of gain in the PID system, which are used to correct or reduce errors, namely K_p , K_i , and K_d . K_p is used to increase the rise time and settling time of the transient response. K_i is used to increasing the steady-state response. K_d is used to improve transient response by predicting future errors. The test was carried out by running the system with different PID parameter values three times to obtain the most optimized-tingling results in maintaining the setpoint at steady state conditions. Based on the results of tests that have been carried out with a setpoint of 40°C, the most optimal results are obtained with values of $K_p=10$, $K_i=20$, and $K_d=30$. The average temperature is 40.02°C with an average error percentage of 2% and an average accuracy rate of 98%.

Keywords: PID, Control System, UV Weathering Chamber.

1. INTRODUCTION

Materials with mechanical properties are related to the material's service life [1]–[3]. Material weathering test is carried out to find out information in determining the material's resistance to the damaging effects of weathering [4]–[6]. Many factors can affect the mechanical properties of a material. UV radiation is one of the key factors in the aging of a material, thus limiting the life of the material [7]. Damage due to UV radiation can be observed as a change in material properties. The influence of high temperature and exposure to ultraviolet (UV) radiation from the sun, rain, and humidity causes damage to the composite material and consequently, reduces its mechanical performance [8], [9].

The effects of ultraviolet radiation are increasingly clear, which can change the properties of materials. The color of the material can change from its original color to become dull and opaque. In addition, the surface shows chalk, cracks, and even erosion. UV radiation can also harden the surface of a material. Weathering test equipment is needed to determine the mechanical properties of material because it

can accelerate the weathering time compared to natural conditions in the open. The device is operated with a programmable control system to provide a simulation of UV weathering. UV simulates the effects of sunlight with an ultraviolet (UV) fluorescent lamp, while rain and dew are simulated by moisture condensation [10], [11].

The degradation of composite materials is affected by UV radiation with the degree of degradation depending on several main parameters such as UV wavelength, exposure time, and UV intensity. This study uses a natural method that takes a long time so it takes a tool to accelerate the degradation time which the tool can regulate the temperature to a certain setpoint. Monitoring the temperature of the room based on Arduino Uno can be a control system for room temperature. The controller helps to run accompanied by controlling the machine [12]–[14].

The operational characteristics of the engine with controller control make the engine performance more optimal [15], [16]. PID control is a type of controller that is very commonly used in the process industry [17]–[20]. Commercial PID modules can generally be found in the form of Special Process

Controller modules (eg temperature controllers, pressure controllers, etc.), DCS modules, or PLC modules [21]–[25]. PID control has 3 types of settings and different functions, namely Proportional Control (P) serves to speed up the response, Integral

Control (I) serves to eliminate steady error, and Derivative Control (D) serves to improve transient response [26]–[29]. Thus, the author will conduct research related to the design of an automatic control system that is used to control the temperature inside the UV Weathering Chamber using a PID Controller. It is hoped that using PID can maintain the temperature at a certain setpoint by tuning PID.

2. MATERIAL AND METHOD

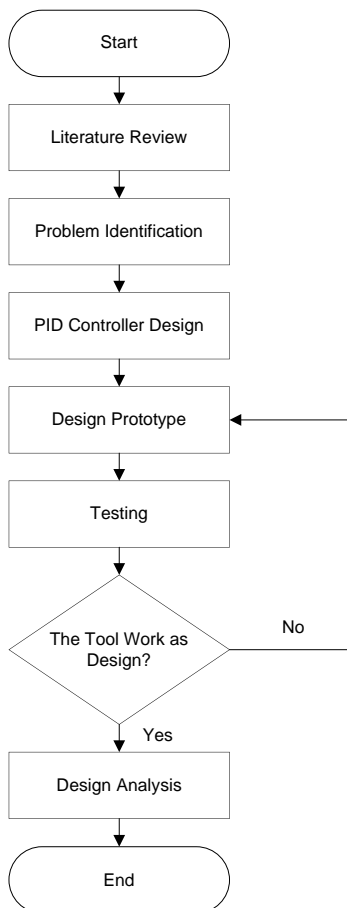


Figure 1. Flowchart of system design

Based on Figure 1 the design process begins with conducting a literature study

related to the problems that occur. At the identification stage of this problem is an analysis of the problems that occur, such as the need for a device design that can control the temperature on the UV Weathering Chamber tool. Then the author finds questions regarding the scope of the problem to be studied so that it can be studied efficiently

A. Design of The System

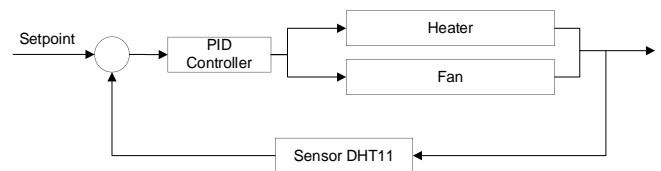


Figure 2. PID system block diagram

In the block diagram Figure 2 has a temperature setpoint, the value of K_p , K_i , and K_d . If the temperature exceeds or is less than a predetermined setpoint, the heater will function to increase the temperature and will turn off when the temperature has reached the setpoint. While the fan to lower temperature if it exceeds the setpoint, besides that the fan also functions to stabilize the temperature during the testing process. PID control is used to control the temperature in the chamber to keep it stable.

The flowchart of the temperature control system that will be made can be seen in Figure 3. When the system is turned on the microcontroller device reads the input and output to be controlled. Then set the temperature setpoint and the length of the test time and the DHT11 sensor reads the temperature in the chamber which will be sent to the microcontroller as input. After receiving the temperature input, the value is processed into a variable using the PID calculation which has the values of K_p , K_i , and K_d . After going through the PID process, the output value is obtained which is used to turn on the heater and fan. When the temperature has reached the setpoint, this program functions continuously during the process to maintain a stable temperature at the setpoint.

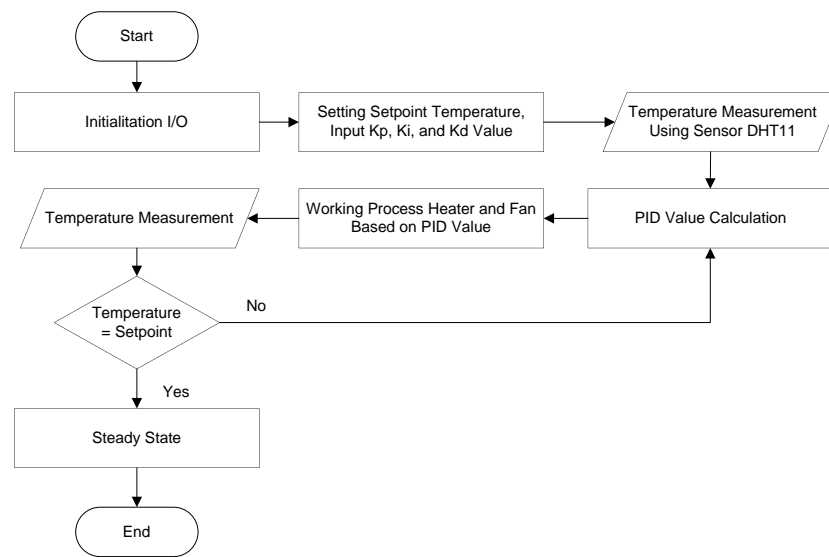


Figure 3. Flowchart system

B. Prototype Design

The prototype design process consists of input and output on the microcontroller. The block diagram of the device in this prototype design can be seen in Figure 4.

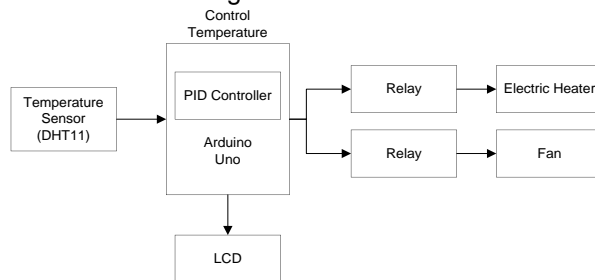


Figure 4. Prototype block diagram

Below are the functions of each section in the block diagram above:

1. Input:
 - a. Temperature Sensor
The sensor is placed in the chamber, it is used to measure the temperature level in the chamber starting before the test until the heater works during the heating process.
2. Output:
 - a. LCD (Liquid Crystal Display)
The LCD is used as an Arduino processing display when setting test parameters and monitoring temperature during the testing process.
 - b. Relay
There are two relays, each of which functions to control the heater and fan components based on orders from Arduino.
 - c. Heater
In designing this prototype using a belt-type heater attached to the chamber

wall. The heater turns on when the temperature in the chamber is below the specified setpoint value and will turn off when it exceeds the temperature setpoint.

d. Fan

Functions as a tool to help lower the temperature, so the fan functions when the temperature exceeds the set point and will turn off during the heating process.

The block diagram explains that it begins with reading the temperature in the chamber by the DHT11 temperature sensor until it is sent to the microcontroller as input and processed using PID. The PID control produces a stable output for system control. The microcontroller sends a command to the relay to turn on the heater to increase the temperature to a predetermined setpoint and the fan to lower and stabilize the temperature in the chamber. The LCD works from the beginning of the sensor reading before the temperature setpoint is determined until it reaches the specified setpoint. As shown in Figure 5 is a prototype control device circuit.



Figure 5. Prototype control

C. Schematic Circuit

The temperature control system design as shown in Figure 6 is divided into several circuits, including the following:

1. Temperature Sensor Circuit as input from the program created
2. Push button circuit as a test parameter controller

3. LCD circuit as a display of the status of the testing process
4. Heater and Fan circuit as the output of data processing from the program created.

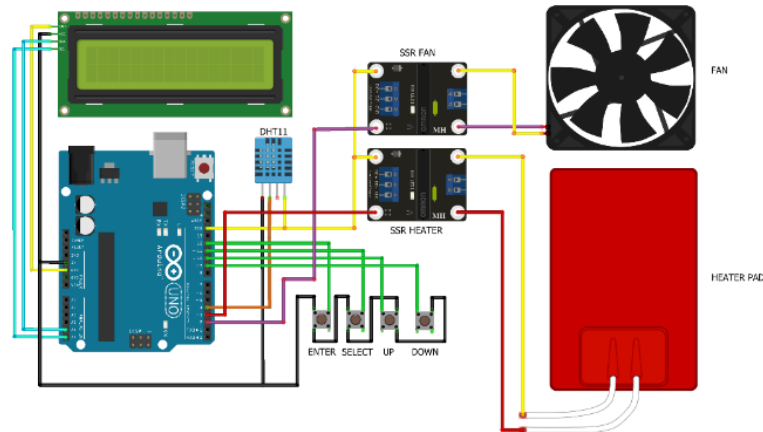


Figure 6. Arduino schematic circuit

DHT11 Temperature Sensor

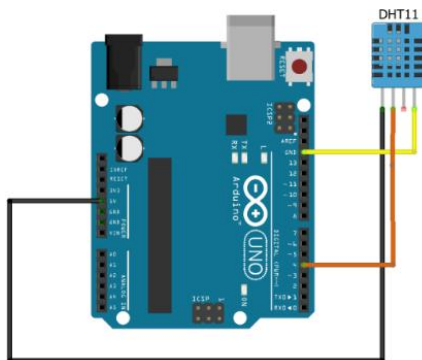


Figure 7. DHT11 sensor circuit

The circuit diagram of the DHT11 sensor which can be seen in Figure 7 is used to read the room temperature inside the prototype device. The results of the sensor readings will be sent to Arduino for processing as input from the program created. command as program output. The connection of the DHT11 sensor pins on the Arduino will be shown in Table 1.

Table 1. DHT11 sensor connection

Pin	Connection
5V Arduino	VCC
Pin 4	DATA
GND	GND
Arduino	

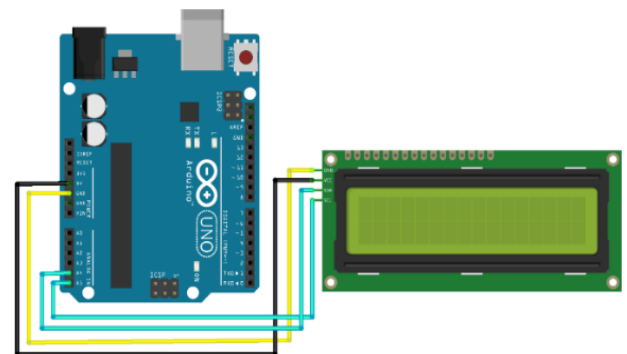


Figure 8. 16x2 LCD circuit

As shown in Figure 8, the LCD connected to the Arduino pin functions to display the testing process starting from the test parameter setup until the testing process takes place. The LCD pin connections on the Arduino can be seen in Table 2.

Table 2. LCD 16X2 connection

Pin	Connection
GND	VCC
Arduino	
5V Arduino	DATA
A4 Arduino	GND
A5 Arduino	SCL

Push Button

Push buttons in the control design that are made are used to set test parameters before the test takes place, 4 push buttons are used as shown in Figure 9. Finding out the connection of the push button pins on the Arduino can be seen in Table 3.

Liquid Crystal Digital (LCD) 16x2

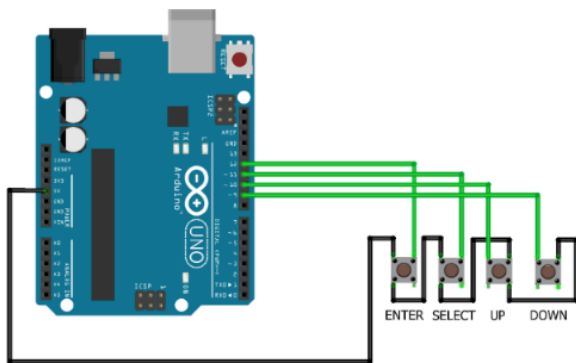


Figure 9. 16x2 LCD circuit

Table 3. Push button connection

Pin	Function
Pin 12	Button ENTER
Pin 11	Button SELECT
Pin 10	Button UP
Pin 9	Button DOWN
5V Arduino	(+)

Heater and Exhaust Fan

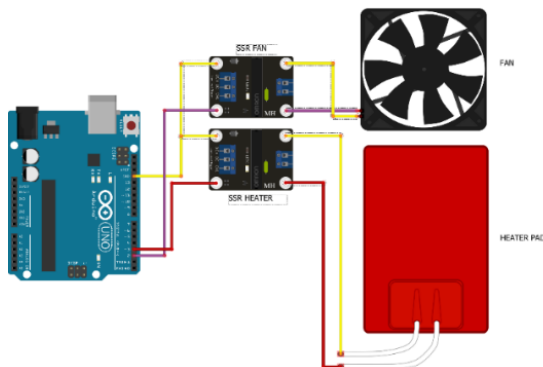


Figure 10. Heater and exhaust fan

The heater and fan are output devices from the control system program created, both devices work when the relay functions are on based on commands that come from the results of microcontroller data processing. As shown in Figure 10, the Heater and Fan are not directly connected to the Arduino but through relay pins. Relay pins connected to Arduino can be seen in Table 4.

Table 4. Heater and fan connection

Pin	Connection
Pin 2	(+) Input VDC Relay Fan
Pin 3	(+) Input VDC Relay Heater
GND Arduino	(-) Input VDC Relay Fan
GND Arduino	(-) Input VDC Relay Heater
(+) Output VAC Relay Fan	(+) Fan
(+) Output VAC Relay Heater	(+) Heater
(-) Output VAC Relay Fan	(-) Fan
(-) Output VAC Relay Heater	(-) Heater

D. Programming Arduino in Arduino IDE

Prototype programming according to the designed scheme is carried out on the Arduino IDE software. PID will control the temperature according to the given setpoint. Based on Figure 11, does not show any errors that occur between the Arduino board connection and the computer and there are no comments that indicate errors in the program.

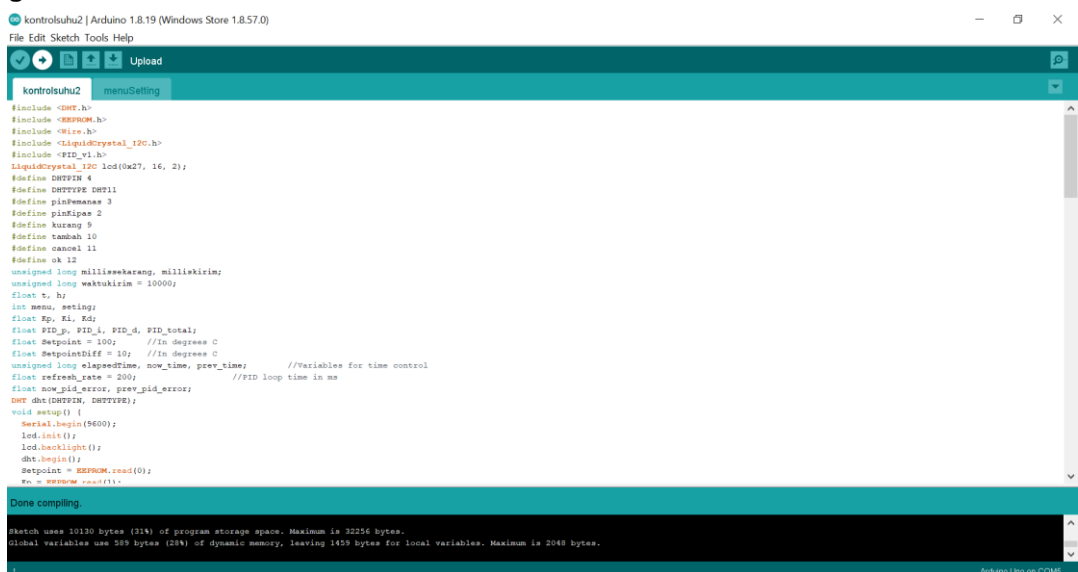


Figure 11. The process of sending data to the arduino board via arduino IDE

3. RESULT AND DISCUSSION

In the research "Design of a Temperature Control System in a PID-Based UV Weathering Chamber" in the test results, there are several categories including, control system hardware test (hardware), device response test to Arduino program, and PID control test to the setpoint temperature.

A. Results of Testing Tools

The results of testing hardware (hardware) there are test indicators, namely:

1. Test LCD 16x2

Figure 12 shows that the LCD is working properly according to the commands given by Arduino. Based on the results of the LCD testing contained in Table 5. that the LCD has worked well according to the commands given by Arduino. The LCD has successfully displayed the test indicator setup display and during the testing process.

Table 5. LCD test results

Test Indicator	Test Criteria	Test Result
Backlight	Light up	Light up
Contrast	Very clear	Very clear
Showing Character	Succeed	Succeed



Figure 12. LCD test results

2. DHT 11 Sensor Test Results

In testing the DHT 11 sensor device, the aim is to determine the sensitivity of the sensor in reading the temperature of the test room. The test is carried out by measuring the temperature in the prototype room using a DHT11 sensor and a comparison measuring instrument using a hygrometer.

Table 6. DHT 11 sensor device test results with hygrometer

DHT 11	Hygrometer	Difference	% Error
27 ⁰ C	27,4 ⁰ C	0,4	1,48
28 ⁰ C	28,9 ⁰ C	0,9	3,21
29 ⁰ C	29,5 ⁰ C	0,5	1,72
30 ⁰ C	30,1 ⁰ C	0,1	0,33
31 ⁰ C	31,7 ⁰ C	0,7	2,26
32 ⁰ C	32,3 ⁰ C	0,3	0,94
33 ⁰ C	33,5 ⁰ C	0,5	1,52
34 ⁰ C	34,9 ⁰ C	0,9	2,65
35 ⁰ C	35,5 ⁰ C	0,5	1,43
36 ⁰ C	36,2 ⁰ C	0,2	0,56
37 ⁰ C	37,9 ⁰ C	0,9	2,43
38 ⁰ C	38,7 ⁰ C	0,7	1,84
39 ⁰ C	39,1 ⁰ C	0,1	0,26
40 ⁰ C	40,5 ⁰ C	0,5	1,25
41 ⁰ C	41,4 ⁰ C	0,4	0,98
<i>X</i> Error		0,51	1,52

Based on the results of the temperature test in Table 6. the results of the percentage error of temperature readings by the DHT 11 sensor and the highest hygrometer are 2.65% and the lowest is 0.26%, with an average error percentage of 1.62%.

B. Response Test Results

The response test was conducted to determine the response relationship between the hardware and the control program in the Arduino program. As shown in Table 7, the results of testing the Arduino program's response to the input given by the pushbutton when setting the test parameters to the display that appears during the heating process and when it has reached overshoot. The test results of all test indicators do not show the occurrence of problems or obstacles so that they can work according to the commands given by Arduino.

Table 7. Test results of device response to arduino program

Test Indicator	Test Criteria	Test Result
Button DOWN	Function	Function
Button UP	Function	Function
Button SELECT	Function	Function
Button ENTER	Function	Function
Display Setup	Function	Function
Parameter	Function	Function
Display Testing	Function	Function
Process	Function	Function
Heater Control	Function	Function
Automatically	Function	Function

C. PID Control Test Against Temperature Setpoint

The control test is carried out to find the PID parameter value that shows optimal results in maintaining the setpoint at a steady state. The test is carried out by setting the PID value parameter on the control panel, then retrieving the test data using the Arduino IDE application which is connected to the Arduino device via a USB 2.0 cable. Figure 13 shows the

temperature measurement data from three tests that show the most optimal results approaching steady state conditions with different PID value parameters. Temperature measurement starts when the temperature passes the setpoint within 30 minutes with an interval of every 1 minute. Below are three tests that show the most optimal results approaching steady-state conditions.

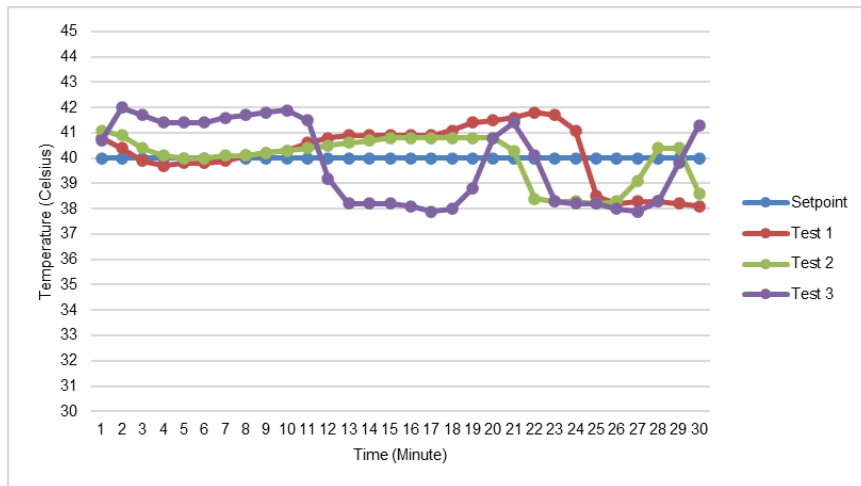


Figure 13. Temperature Test Results

Based on the test graph above, shows fluctuating results, from the three tests show similar results. This is influenced by several factors, including the density level of the prototype testing tool and the heater power which is too small compared to the volume of the prototype testing tool. To find out the most optimal test results, it is necessary to find the average temperature that is closest to the temperature setpoint which is then used from

the test data to find the percentage error and maximum overshoot. Based on the test data, the most optimal results in "Design of Temperature Control System on UV Weathering Chamber Based on PID" were found in the second experiment with parameter values $K_p=10$, $K_i=20$, and $K_d=30$. The second test graph can be seen in Figure 14.

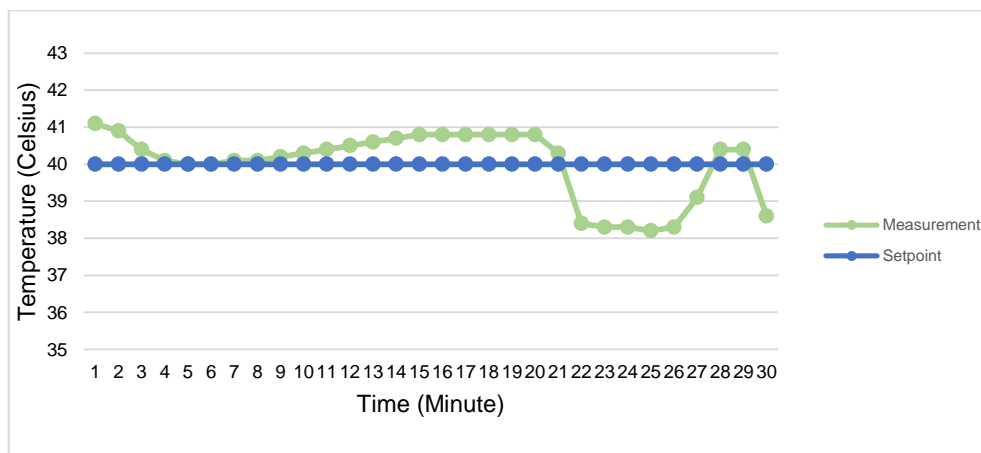


Figure 14. The Second Test Results

Based on the graph in Figure 14 the peak temperature occurs at 41.1⁰C. The average temperature obtained is 40.02⁰C which is the closest to the setpoint value. So, the temperature measurement data in the second test is used as a reference to find the next calculation

$$\% \text{ Error} = \frac{|T_{\text{Measurement}} - T_{\text{Setpoint}}|}{T_{\text{Setpoint}}} \times 100\% \quad (1)$$

From the error calculation formula, the average error percentage is 2% and the average accuracy is 98%.

The calculation of the percentage value of overshoot is obtained from the following:

$$\% \text{ Overshoot} = \frac{T_{\text{Peak}} - T_{\text{Setpoint}}}{T_{\text{Setpoint}}} \times 100\% \quad (2)$$

$$\% \text{ Overshoot} = \frac{41.1 - 40}{40} \times 100\% = 2.75 \%$$

4. CONCLUSION

Based on the results of the study, it can be concluded that the prototype device for the PID control system functions well, can work according to the commands given, and based on the analysis above, which was carried out 3 times, the results obtained are fluctuating graph readings with parameters $K_p = 10$, $K_i = 20$, $K_d = 30$ the average error percentage is 2% and the overshoot value is 2.75%. The PID control system works influenced by the changing ambient room temperature, the power on the heater used is too small when compared to the volume of the testing prototype tool room, and the density of the testing prototype tool room. the research "Design of a Temperature Control System in a PID-Based UV Weathering Chamber" in the test results, there are several categories including, control system hardware test (hardware), device response test to Arduino program, and PID control test to the setpoint temperature.

5. ACKNOWLEDGMENTS

The authors would like to thank Mercur Buana University for their support through the founding of this research.

REFERENCES

- [1] D. Sebayang *et al.*, "Numerical simulation of distortion and phase transformation in laser welding process using MSC Marc/Mentat," *IOP Conf. Ser. Mater. Sci. Eng.*, vol. 453, no. 1, 2018, doi: 10.1088/1757-899X/453/1/012020.
- [2] F. Anggara, D. Romahadi, A. L. Avicenna, and Y. H. Irawan, "Numerical analysis of the vortex flow effect on the thermal-hydraulic performance of spray dryer," *SINERGI*, vol. 26, no. 1, pp. 23–30, Feb. 2022, doi: 10.22441/SINERGI.2022.1.004.
- [3] D. Romahadi, N. Ruhyat, and L. B. D. Dorion, "Condensor design analysis with Kays and London surface dimensions," *SINERGI*, vol. 24, pp. 81–86, 2020, doi: 10.22441/sinergi.2020.2.001.
- [4] J. Qin *et al.*, "Sunlight tracking and concentrating accelerated weathering test applied in weatherability evaluation and service life prediction of polymeric materials: A review," *Polym. Test.*, vol. 93, p. 106940, Jan. 2021, doi: 10.1016/J.POLYMERTESTING.2020.106940.
- [5] S. Cesari, G. Emmi, and M. Bottarelli, "A weather forecast-based control for the improvement of PCM enhanced radiant floors," *Appl. Therm. Eng.*, vol. 206, p. 118119, Apr. 2022, doi: 10.1016/J.APPLTHERMALENG.2022.118119.
- [6] M. Hu, G. Sun, D. Sun, T. Lu, J. Ma, and Y. Deng, "Accelerated weathering simulation on rheological properties and chemical structure of high viscosity modified asphalt: A temperature acceleration effect analysis," *Constr. Build. Mater.*, vol. 268, p. 121120, Jan. 2021, doi: 10.1016/J.CONBUILDMAT.2020.121120.
- [7] M. Jamal, G. Martinez-Arguelles, and F. Giustozzi, "Effect of waste tyre rubber size on physical, rheological and UV resistance of high-content rubber-modified bitumen," *Constr. Build. Mater.*, vol. 304, p. 124638, Oct. 2021, doi: 10.1016/J.CONBUILDMAT.2021.124638.
- [8] P. Sanmartín and J. S. Pozo-Antonio, "Weathering of graffiti spray paint on building stones exposed to different types of UV radiation," *Constr. Build. Mater.*, vol. 236, p. 117736, Mar. 2020, doi: 10.1016/J.CONBUILDMAT.2019.117736.
- [9] R. F. Nascimento, A. O. da Silva, R. P. Weber, and S. N. Monteiro, "Influence of UV radiation and moisture associated with natural weathering on the ballistic performance of aramid fabric armor," *J. Mater. Res. Technol.*, vol. 9, no. 5, pp. 10334–10345, Sep. 2020, doi: 10.1016/J.JMRT.2020.07.046.

- [10] G. F. L. R. Bernardes, R. Ishibashi, A. A. S. Ivo, V. Rosset, and B. Y. L. Kimura, "Prototyping low-cost automatic weather stations for natural disaster monitoring," *Digit. Commun. Networks*, May 2022, doi: 10.1016/J.DCAN.2022.05.002.
- [11] M. Fitri, T. Susilo, D. Feriyanto, and D. M. Zago, "Effect Of morphology and percentage of second phase content of coconut coir on the impact strength of epoxy resin composites," *Nat. Volatiles Essent. Oils*, vol. 8, no. 6, pp. 3880–3894, 2021.
- [12] D. Romahadi, F. Anggara, A. F. Sudarma, and H. Xiong, "The implementation of artificial neural networks in designing intelligent diagnosis systems for centrifugal machines using vibration signal," *SINERGI*, vol. 25, no. November 2020, 2021, doi: 10.22441/sinergi.2021.1.012.
- [13] D. Romahadi, A. A. Luthfie, W. Suprihatiningsih, and H. Xiong, "Designing expert system for centrifugal using vibration signal and Bayesian Networks," *Int. J. Adv. Sci. Eng. Inf. Technol.*, vol. 12, no. 1, p. 23, Jan. 2022, doi: 10.18517/IJASEIT.12.1.12448.
- [14] Irianto, F. D. Murdianto, E. Sunarno, and Yusra, "Robustness analysis of speed control method to drive AC/DC motor," *Int. J. Adv. Sci. Eng. Inf. Technol.*, vol. 11, no. 5, pp. 1794–1800, 2021, doi: 10.18517/ijaseit.11.5.9575.
- [15] D. Romahadi, H. Xiong, and H. Pranoto, "Intelligent system for gearbox fault detection & diagnosis based on vibration analysis using Bayesian Networks," *IOP Conf. Ser. Mater. Sci. Eng.*, vol. 694, no. 1, 2019, doi: 10.1088/1757-899X/694/1/012001.
- [16] D. Romahadi, F. Anggara, R. P. Youlia, H. L. Habibullah, and H. Xiong, "Bayesian networks approach on intelligent system design for the diagnosis of heat exchanger," *SINERGI*, vol. 26, no. 2, pp. 127–136, May 2022, doi: 10.22441/SINERGI.2022.2.001.
- [17] M. H. Suid and M. A. Ahmad, "Optimal tuning of sigmoid PID controller using Nonlinear Sine Cosine Algorithm for the Automatic Voltage Regulator system," *ISA Trans.*, Dec. 2021, doi: 10.1016/J.ISATRA.2021.11.037.
- [18] A. Kherkhar, Y. Chiba, A. Tlemçani, and H. Mamur, "Thermal investigation of a thermoelectric cooler based on Arduino and PID control approach," *Case Stud. Therm. Eng.*, vol. 36, p. 102249, Aug. 2022, doi: 10.1016/J.CSITE.2022.102249.
- [19] B. S. Taysom, C. D. Sorensen, and J. D. Hedengren, "A comparison of model predictive control and PID temperature control in friction stir welding," *J. Manuf. Process.*, vol. 29, pp. 232–241, Oct. 2017, doi: 10.1016/J.JMAPRO.2017.07.015.
- [20] J. L. Song, W. L. Cheng, Z. M. Xu, S. Yuan, and M. H. Liu, "Study on PID temperature control performance of a novel PTC material with room temperature Curie point," *Int. J. Heat Mass Transf.*, vol. 95, pp. 1038–1046, Apr. 2016, doi: 10.1016/J.IJHEATMASSTRANSFER.2015.12.057.
- [21] H. H. Manap, A. K. Abdul Wahab, and F. Mohamed Zuki, "Control for Carbon Dioxide Exchange Process in a Membrane Oxygenator Using Online Self-Tuning Fuzzy-PID Controller," *Biomed. Signal Process. Control*, vol. 64, p. 102300, Feb. 2021, doi: 10.1016/J.BSPC.2020.102300.
- [22] M. Schiavo, F. Padula, N. Latronico, M. Paltenghi, and A. Visioli, "Individualized PID Tuning for Maintenance of General Anesthesia with Propofol," *IFAC-PapersOnLine*, vol. 54, no. 3, pp. 679–684, Jan. 2021, doi: 10.1016/J.IFACOL.2021.08.320.
- [23] X. Yu, X. Yang, C. Yu, J. Zhang, and Y. Tian, "Direct approach to optimize PID controller parameters of hydropower plants," *Renew. Energy*, vol. 173, pp. 342–350, Aug. 2021, doi: 10.1016/J.RENENE.2021.03.129.
- [24] B. Arun, B. V. Manikandan, and K. Premkumar, "Multiarea Power System Performance Measurement using Optimized PID Controller," *Microprocess. Microsyst.*, p. 104238, Feb. 2021, doi: 10.1016/J.MICPRO.2021.104238.
- [25] H. Liang, Z. K. Sang, Y. Z. Wu, Y. H. Zhang, and R. Zhao, "High precision temperature control performance of a PID neural network-controlled heater under complex outdoor conditions," *Appl. Therm. Eng.*, vol. 195, p. 117234, Aug. 2021, doi: 10.1016/J.APPLTHERMALENG.2021.117234.
- [26] A. Kumar and S. Pan, "Design of fractional order PID controller for load frequency control system with communication delay," *ISA Trans.*, Dec. 2021, doi: 10.1016/J.ISATRA.2021.12.033.
- [27] M. Ma, H. Wang, N. Xiang, P. Yun, and H.

- Wang, "Fault diagnosis of PID in crystalline silicon photovoltaic modules through I-V curve," *Microelectron. Reliab.*, vol. 126, p. 114236, Nov. 2021, doi: 10.1016/J.MICROREL.2021.114236.
- [28] P. Z. Csurcsia, P. Bhandari, and T. De Troyer, "Development of a low-cost PID setup for engineering technology students," *IFAC-PapersOnLine*, vol. 55, no. 4, pp. 213–218, Jan. 2022, doi: 10.1016/J.IFACOL.2022.06.035.
- [29] S. S. Franco, J. R. Henríquez, A. A. V. Ochoa, J. A. P. da Costa, and K. A. Ferraz, "Thermal analysis and development of PID control for electronic expansion device of vapor compression refrigeration systems," *Appl. Therm. Eng.*, vol. 206, p. 118130, Apr. 2022, doi: 10.1016/J.APPLTHERMALENG.2022.118130.